JACS
JOURNAL OF THE AMERICAN CHEMICAL SOCIETY
Article
pubs.acs.org/JACS

Selective Preparation of Macroporous Monoliths of Conductive Titanium Oxides Ti_nO_{2n-1} (n = 2, 3, 4, 6)

Atsushi Kitada,[†,#] George Hasegawa,[‡,#] Yoji Kobayashi,[†] Kazuyoshi Kanamori,[‡] Kazuki Nakanishi,[‡] and Hiroshi Kageyama*[,†,¶,§]

[†]Department of Energy and Hydrocarbon Chemistry, Graduate School of Engineering, Kyoto University, Nishikyo-ku, Kyoto 615-8510, Japan

[‡]Department of Chemistry, Graduate School of Science, Kyoto University, Kitashirakawa, Sakyo-ku, Kyoto 606-8502, Japan

[¶]Institute for Integrated Cell-Material Sciences (iCeMS), Kyoto University, Yoshida-Ushinomiya, Sakyo-ku, Kyoto 606-8501

[§]CREST, Japan Science and Technology Agency (JST), Kawaguchi, Saitama 332-0012, Japan

Supporting Information

ABSTRACT: Monolithic conductive titanium oxides Ti_nO_{2n-1} (n = 2, 3, 4, 6) with well-defined macropores have been successfully prepared as a single phase, via reduction of a macroporous TiO_2 precursor monolith using zirconium getter. Despite substantial removal of oxide ions, all the reduced monoliths retain the macropore properties of the precursor, i.e., uniform pore size distribution and pore volume. Furthermore, compared to commercial porous Ebonex (shaped conductive Ti_nO_{2n-1}), the bulk densities (1.8 g cm^{-3}) are half, and the porosities (60%) are about 3 times higher. The obtained Ti_nO_{2n-1} (n = 2, 3, 4, 6) macroporous monoliths could find applications as electrodes for many electrochemical reactions.

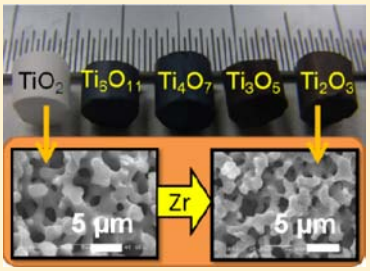

1. INTRODUCTION

Titanium oxides generally feature low environmental burden, biocompatibility, low cost, and chemical stability. Titanium dioxide ($Ti(IV)O_2$; d^0), as a wide-gap semiconductor, exhibits photocatalytic and photovoltaic properties.[1,2] Reduced titanium oxides with d electrons are also attractive regarding transport and magnetic properties; a series of reduced titanium oxides (Ti_nO_{2n-1}; n = 2, 3, 4, ..., 10) undergo Peierls-like metal−insulator transitions, which can be controlled by external stimuli such as temperature, light, and pressure,[3−5] and therefore might be useful for memory and switching devices. Ti_4O_7 (n = 4) finds applications as electrodes for electrochemical reactions.[6,7]

Porous oxides receive considerable attention because of their good mass transport, high surface area, and low density. In particular, when they are of monolithic form, various applications can be found, including electrodes,[6−8] separation media,[9,10] biomedical materials,[11] and so on. Such porous oxide monoliths have usually been prepared via the sol−gel process, by polymer or silica template methods,[6−8,12−15] or by phase separation.[9,10,16−22] Among the methods currently available, phase separation based on spinodal decomposition allows precise control of pore properties (e.g., pore size and pore volume). In addition, it is a simple method that requires adjusting starting compositions and does not require any templates.

Ever since the first report on porous silica monoliths, various kinds of porous oxide monoliths with well-controlled pore properties have been synthesized using phase separation based on spinodal decomposition.[23] Examples include aluminum oxides (Al_2O_3 and $Y_3Al_5O_{12}$),[17,18] titanium oxides (TiO_2 and $ATiO_3$ (A = Ca, Sr, Ba)),[19−21] and zirconium oxide (ZrO_2).[22] However, all of these oxide monoliths are insulators. Therefore, a conductive porous oxide monolith with controlled porosity is an appealing system because it would open an avenue for electrochemical applications such as electrodes or catalysts, which have been so far almost exclusively limited to carbonaceous materials. As far as the authors know, porous monoliths of conductive oxides have been reported only for Ti_4O_7 (commercially available as Ebonex from Atraverda Ltd.) and $(La,Sr)MnO_3$, relying on different synthesis strategies; the former is prepared by thermal decomposition of TiO_2 powder and polymer binders, followed by H_2 reduction,[6,7,24] while the latter is prepared by heat treatment of a mixture of K_2CO_3, $MnSO_4{\cdot}5H_2O$, La_2O_3, and $SrCO_3$, followed by water rinsing to eliminate K_2SO_4.[25] Unfortunately, in either case it is impossible to precisely control their pore properties.

In this paper we report on the selective synthesis, with a zirconium getter, of a series of conductive titanium oxide porous monoliths. As a precursor, we used an anatase-type TiO_2 monolith with interconnected and well-defined macropores, prepared recently via a phase separation method.[20] Depending on the amount of Zr and the reaction temperature, the TiO_2 monoliths convert to a single phase of Ti_6O_{11}, Ti_4O_7, Ti_3O_5, and Ti_2O_3, with retained macropore properties of the precursor. Namely, all the obtained monoliths have a uniform pore size distribution and relatively large porosity of about 60%.

Received: March 2, 2012
Published: June 11, 2012

 © 2012 American Chemical Society dx.doi.org/10.1021/ja302083n | J. Am. Chem. Soc. 2012, 134, 10894−10898

2. EXPERIMENTAL PROCEDURES

2.1. Reagents. Titanium(IV) *n*-propoxide ($Ti(O^nPr)_4$) and polyethylene glycol (PEG, M_w = 10 000) were purchased from Sigma-Aldrich Co. (Madison, WI). Ethyl acetoacetate (EtAcAc) and 1-propanol (PrOH) were purchased from Tokyo Chemical Industry Co., Ltd., whereas NH_4NO_3 was obtained from Kishida Chemical Co., Ltd. Ziconium foil (99.2% purity, 0.1 mm in thickness) was purchased from Rare Metallic Co. All reagents were used as received. Distilled water was used in all experiments.

2.2. Preparation of the Porous TiO_2 Precursor Monoliths. Porous TiO_2 monoliths were prepared according to the sol–gel method reported previously.[20] In a typical preparation, $Ti(O^nPr)_4$ (2.0 mL), PrOH (1.4 mL), and EtAcAc (1.0 mL) were mixed in a glass tube. After obtaining a homogeneous yellow solution, PEG (0.175 g) was added, and the solution was stirred at 60 °C until PEG was completely dissolved. The solution was then cooled to 40 °C, and 1 M NH_4NO_3 aqueous solution (0.4 mL) was added slowly with vigorous stirring. After mixing for 3 min, the obtained homogeneous solution was kept at 40 °C for 24 h. The obtained gels were washed with ethanol at 60 °C, followed by a stepwise solvent exchange from ethanol to H_2O. The resultant gels were finally immersed in H_2O at 60 °C for 24 h. After drying of the wet gels at 40 °C, the resultant xerogels were calcined at 600 °C/800 °C for 2 h, resulting in anatase/rutile structure.

2.3. Preparation of the Porous Ti_nO_{2n-1} Monoliths. The reduction of the monolith with elemental zirconium leads to Ti_nO_{2n-1} (n = 2, 3, 4, and 6), which can be expressed as

$$2nTiO_2 + Zr \rightarrow 2Ti_nO_{2n-1} + ZrO_2$$

The anatase TiO_2 monolith (typically 5 mm in diameter, 5 mm in height) was placed in an evacuated ($< 4 \times 10^{-2}$ Pa) quartz tube, separated by approximately 5 mm from a piece of Zr foil (99.2% purity, 0.1 mm in thickness). In all the reaction conditions we attempted, a reaction time of 1 day and heating/cooling rates of 100 °C/h were employed, while the ratio of TiO_2: Zr was varied corresponding to the reaction equation with 0–10% excess of Zr, and the reaction temperatures were changed between 1000 and 1180 °C.

2.4. Characterization. Powder X-ray diffraction (XRD) profiles were obtained using a Bruker D8 diffractometer with Cu Kα (λ = 0.154 nm) radiation as the incident beam. Transmission electron microscopy (TEM) was performed on a Hitachi H-9000 instrument operating at 300 kV. Scanning electron microscopy (SEM) was performed on JEOL JSM-6060S and JSM-6700F instruments. The electrical resistivity of each specimen was measured by the four-probe method using a Physical Property Measurement System (PPMS, Quantum Design, USA). N_2 adsorption–desorption apparatus (Belsorp mini II, Bel Japan Inc.) was employed to characterize meso- and micropores. A mercury porosimeter (Pore Master 60-GT, Quantachrome Instruments, Boynton Beach, FL) was used to characterize the macropores of the samples, while helium pycnometry (Accupyc 1330, Micromeritics, Norcross, GA) was employed to determine the skeletal density of the samples. The bulk density was calculated from the weight and volume calculated from precisely measured dimensions of each specimen. The porosity (%) of each sample was calculated as $[(1 - d_b)/d_s] \times 100$, where d_b and d_s are assigned as the bulk and skeletal densities, respectively.

3. RESULTS AND DISCUSSION

3.1. Preparation of the Porous Ti_nO_{2n-1} Monoliths. Typical reaction conditions are listed in Table S1. In all cases, a reaction time of 1 day and heating/cooling rates of 100 °C/h were employed. The use of a stoichiometric TiO_2/Zr ratio in the reaction equation always resulted in a contamination of less-reduced (i.e., larger n) phases, together with the target phase, due to incomplete oxidation of Zr to ZrO_2. For example, for TiO_2:Zr = 12 (corresponding to n = 6), thermal treatment at 1050 °C yielded a Ti_6O_{11} and Ti_7O_{13} mixture. Therefore, in order to isolate the Ti_6O_{11} phase, we used a 10% excess amount of Zr to compensate for incomplete oxidation (see Figure S1). We also found that what products are formed depends on the reaction temperature. For example, with a molar ratio of TiO_2:Zr = 6:1.05 ($n \approx 3$), reactions at 1100, 1150, and 1180 °C resulted in a single phase of Ti_4O_7 (n = 4), a single phase of Ti_3O_5 (n = 3), and mixed phases of Ti_2O_3 (n = 2) and Ti_3O_5 (n = 3), respectively (see Figure S2). In summary, the typical requirements to obtain single phases are a 5% Zr excess for Ti_2O_3, Ti_3O_5, and Ti_4O_7, and 10% for Ti_6O_{11}, and reaction temperatures of 1150 °C for Ti_2O_3 and Ti_3O_5, and 1050 °C for Ti_4O_7 and Ti_6O_{11}.

It is highly remarkable that, as displayed in Figure 1, the thus obtained compounds Ti_2O_3, Ti_3O_5, Ti_4O_7, and Ti_6O_{11} retain

Figure 1. Photograph of anatase TiO_2, Ti_6O_{11}, Ti_4O_7, Ti_3O_5, and Ti_2O_3 monoliths (from left to right).

their monolithic shape without noticeable changes in diameter and height and without any visible cracks. The reduced Ti_nO_{2n-1} monoliths have an interconnected macropore network with uniform pore size of about 2 μm and relatively high porosity of about 60%, similar to the anatase TiO_2 precursors. Furthermore, reflecting the color change from white to black, they have relatively low electrical resistivities of 10^1–10^{-2} Ω cm at room temperature (RT). Details of the pore and transport properties will be discussed later.

3.2. Characterization of Ti_nO_{2n-1} Macroporous Monoliths. Figure 2 exhibits observed and calculated XRD profiles of

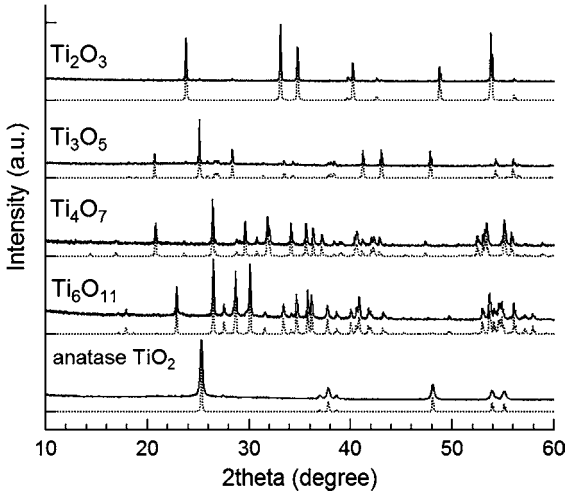

Figure 2. Observed (solid lines) and calculated (dotted lines) XRD profiles of anatase TiO_2, Ti_6O_{11}, Ti_4O_7, Ti_3O_5, and Ti_2O_3 monoliths (from bottom to top).

the precursor anatase TiO_2 and its reduced products Ti_nO_{2n-1}, with n = 2, 3, 4, 6. The XRD peaks for anatase TiO_2 are broad (fwhm = 0.276°, for the peak at 25.3°) due to the small crystallite size. Using Scherrer's equation, the crystallite size was estimated as ~32 nm, which is consistent with TEM results (20–60 nm), as shown in Figure S3a. In contrast, the XRD peaks for the reduced phases are relatively sharp (fwhm = 0.143° (n = 6), 0.123° (n = 4), 0.098° (n = 3), and 0.062° (n =

dx.doi.org/10.1021/ja302083n | J. Am. Chem. Soc. 2012, 134, 10894–10898

2), for the peaks at 26.5°, 26.4°, 25.1°, and 23.8°, respectively), indicating crystallite growth. After accounting for instrumental broadening, the estimated crystallite sizes are 67 nm for $n = 6$, 83 nm for $n = 4$, and 119 nm for $n = 3$. For $n = 2$, the fwhm is virtually the same as instrumental broadening (fwhm = 0.06°), signifying sintering to large particle sizes beyond the Scherrer range. TEM and SEM (Figures S3b, S4) show that the crystallites are indeed intimately fused or even consolidated to form large single-crystal particles on the micrometer scale. Each XRD pattern of reduced phases resembles the corresponding simulated one without impurities, and the lattice parameters are in excellent agreement with the reported values.[26−29] Notably, commercial Ebonex is not a single phase, but a mixture of Ti_4O_7 and Ti_5O_9.[6] The electrical resistivity data for our Ti_4O_7 and Ti_6O_{11} monoliths exhibit anomalies which are associated with the Peierls-like metal−insulator transition at $T_{MI} \approx 150$ K and $T_{MI} \approx 170$ K, respectively (Figure 3a), while those for the

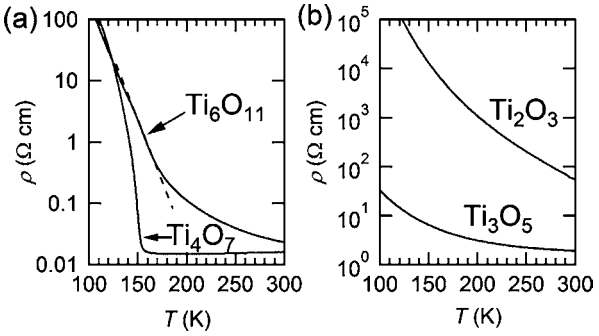

Figure 3. Temperature dependence of electrical resistivity for (a) Ti_4O_7 and Ti_6O_{11} and for (b) Ti_2O_3 and Ti_3O_5. The dotted line in (a) is a guide to the eye.

Ti_3O_5 and Ti_2O_3 monoliths exhibit semiconducting behavior below 300 K (Figure 3b). This is similar to the previous reports on single-crystalline Ti_nO_{2n-1},[4,30,31] although the observed anomalies for the Ti_6O_{11} and Ti_4O_7 monoliths were less sharp due to the polycrystalline nature.

When a rutile TiO_2 precursor was used instead of anatase, we were not able to isolate any of the reduced phases by the Zr getter. Here, the rutile TiO_2 precursor was prepared by calcining the dried TiO_2 gels at 800 °C for 2 h in air.[20] At the reaction conditions where anatase TiO_2 transformed to Ti_6O_{11}, the rutile precursor resulted in a mixture of Ti_4O_7, Ti_5O_9, and Ti_6O_{11}. Such a difference was also seen when attempting to synthesize a single phase of Ti_nO_{2n-1} ($n = 2, 3, 4$) from rutile (see Figure S5). However, these observations do not mean that the *direct* transformation from the metastable anatase to any of the reduced phases is essential for isolating a single-phase monolith. We have confirmed in a separate quenching experiment that, in preparing the reduced phases from the anatase precursors, a rutile intermediate is indeed encountered (see Figure S6). However, the extended treatment at 800 °C experienced by the explicitly prepared rutile monolith probably leads to the different reduction behavior.

It is remarkable that, despite substantial removal of oxide ions and the non-topochemical transformation of lattice frameworks, the macropore properties of the anatase TiO_2 monolith are retained during the reduction. Figure 4a−e shows SEM images of anatase TiO_2 precursor, Ti_6O_{11}, Ti_4O_7, Ti_3O_5, and Ti_2O_3, respectively. All the images of the reduced oxides demonstrate interconnected pore structures, similar to that of

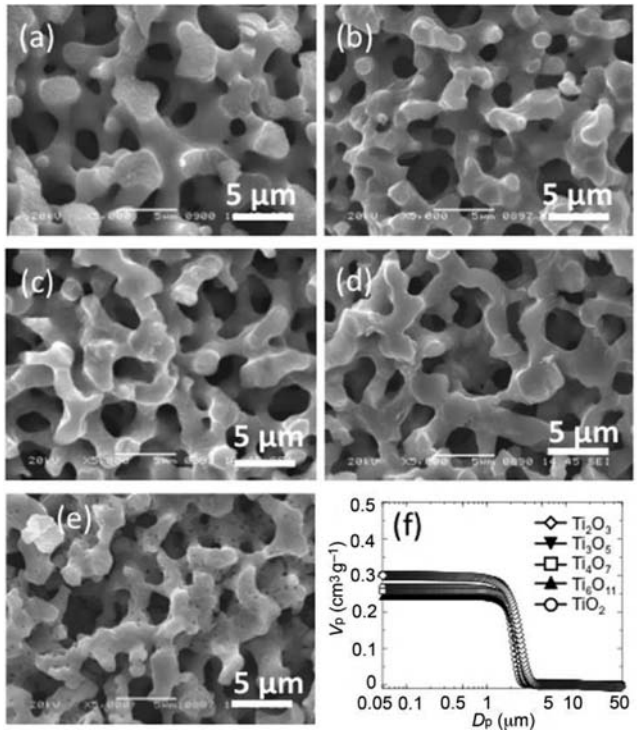

Figure 4. SEM images of macroporous monoliths of (a) anatase TiO_2, (b) Ti_6O_{11}, (c) Ti_4O_7, (d) Ti_3O_5, and (e) Ti_2O_3. (f) Mercury porosimetry results of anatase TiO_2, Ti_6O_{11}, Ti_4O_7, Ti_3O_5, and Ti_2O_3.

the precursor. In Ti_2O_3, the most reduced material, pinhole-like pores are seen on the surface. Mercury porosimetry measurements as shown in Figure 4f demonstrate that all materials possess uniform macropores of around 2 μm; in addition, the macropore diameter and volume are almost the same in all samples, which indicates that the well-defined macroporous structure of the precursor monolith was retained. N_2 physisorption results are shown in Figure S7. The anatase TiO_2 monolith had some micro- and mesopores as reported previously, and a BET surface area of 20 $m^2\ g^{-1}$.[20] In contrast, only a small amount of meso- and micropores remained in the reduced Ti_nO_{2n-1} monoliths due to sintering. Therefore, the observed pinholes in Ti_2O_3 (Figure 4e) are not mesopores of any notable significance.

Table 1 summarizes the densities, porosities, and electrical resistivities at RT of the obtained monoliths and a commercial porous product, Ebonex, made from Ti_4O_7/Ti_5O_9.[6] The skeletal densities of the anatase precursor (3.83 g cm^{-3}) and the Ti_nO_{2n-1} monoliths (4.25−4.38 g cm^{-3}) agree well with the expected densities (3.89 and 4.25−4.57 g cm^{-3}) calculated from previous reports.[26−29] Moreover, the bulk density of each porous Ti_nO_{2n-1} material is estimated to be 1.75−1.85 g cm^{-3}, and gives a porosity as large as 57−60%, which is close to that of the precursor (64%). To the best of our knowledge, such low bulk densities and large porosities have not been reported in porous monoliths of reduced titanium oxides; for example, the commercially available Ebonex has a bulk density about 2 times higher (3.6−3.8 g cm^{-3}) and a porosity about 3 times smaller (20%).[6] Furthermore, all the reduced monoliths have relatively low electrical resistivities in the range of 10^1−10^{-2} Ω cm at RT (see Table 1). In particular, the RT resistivity of the Ti_4O_7 porous monolith is 1.5×10^{-2} Ω cm, lower than that of porous

dx.doi.org/10.1021/ja302083n | J. Am. Chem. Soc. 2012, 134, 10894−10898

Table 1. Pore Characteristics and Transport Properties of the Reduced Ti_nO_{2n-1}, Anatase TiO_2, and a Commercial Porous Ebonex at Room Temperature

sample[a]	d_s[b] (g cm^{-3})	d_t[c] (g cm^{-3})	d_b[d] (g cm^{-3})	porosity[e] (%)	ρ[f] (Ω cm)
Ti_2O_3	4.38	4.57	1.75	60	5.6×10^{1}
Ti_3O_5	4.25	4.25	1.78	58	1.9×10^{0}
Ti_4O_7	4.33	4.32	1.82	58	1.5×10^{-2}
Ti_6O_{11}	4.28	4.30	1.85	57	2.0×10^{-2}
TiO_2	3.83	3.89	1.39	64	–
porous Ebonex	–	–	3.6–3.8	20	2.0×10^{-2}

[a]Data for porous Ebonex obtained from ref 6. [b]Skeletal density measured by helium pycnometry. [c]Reported true density.[26−29] [d]Bulk density calculated from the weight and volume obtained from precisely measured dimensions of each specimen. [e]Calculated by $[(1 - d_b)/d_s] \times 100$. [f]Bulk electrical resistivity.

Ebonex (2×10^{-2} Ω cm), where a less conductive Ti_5O_9 exists as a secondary phase.[6]

Compared to carbon electrodes, Ebonex electrodes have higher corrosion resistance at very positive and negative potentials and have been commercially utilized in bipolar batteries.[6,7] Ebonex has also been studied in terms of oxygen/hydrogen evolution and/or oxygen reduction for fuel cells, and oxidation of harmful molecules such as sulfur dioxide and halogenated organic species in aqueous waste solutions.[32−37] The obtained Ti_nO_{2n-1} macroporous monoliths, which have much lower bulk densities and much larger porosities than the commercial porous Ebonex, may be useful for many applications. Notably, the success in the selective preparation of Ti_2O_3, Ti_3O_5, Ti_4O_7, and Ti_6O_{11}, each as a single phase, provides an opportunity to compare the support effect of each Ti_nO_{2n-1} porous monolith when used as a catalyst support. Thus, further electrochemical investigation is required for the obtained macroporous Ti_nO_{2n-1} monoliths.

4. CONCLUSIONS

We report the selective preparation of macroporous monoliths of titanium oxides Ti_nO_{2n-1}, with n = 2 (Ti_2O_3), 3 (Ti_3O_5), 4 (Ti_4O_7), and 6 (Ti_6O_{11}), by simply reducing macroporous anatase TiO_2 monoliths using a zirconium getter. Despite substantial removal of oxide ions and non-topochemical transformation of lattice frameworks, the obtained monoliths have macropore properties similar to those of the TiO_2 precursor (i.e., uniform pore size and large porosities up to 60%). The obtained porous Ti_nO_{2n-1} monoliths with high conductivities and low densities could find various electrochemical applications. Notably, porous Ti_nO_{2n-1} with different pore sizes can be obtained because the macropores of the TiO_2 precursors are easily controlled using the phase separation method.[20] Moreover, starting from porous TiO_2 monoliths, various kinds of conductive materials such as (oxy)nitrides and carbides could be prepared that retain the pore properties of the precursor.

■ ASSOCIATED CONTENT

Supporting Information

List of typical reaction conditions, TEM and SEM images, and XRD patterns of the samples. This material is available free of charge via the Internet at http://pubs.acs.org.

■ AUTHOR INFORMATION

Corresponding Author

kage@scl.kyoto-u.ac.jp

Author Contributions

#A.K. and G.H. contributed equally.

Notes

The authors declare no competing financial interest.

■ ACKNOWLEDGMENTS

This work was supported by Grant-in-Aid for Scientific Research (A) (No. 22245009) and Grant-in-Aid for Research Activity (No. 22750203) from MEXT, and by CREST from JSPS (Japan). A.K. and G.H. were supported by Japan Society for the Promotion of Science for Young Scientists.

■ REFERENCES

(1) Fujishima, A.; Zhang, X. *C. R. Chim.* **2005**, *9*, 750.
(2) O'Regan, B.; Gratzel, M. *Nature* **1991**, *353*, 737.
(3) Ohkoshi, S.; Tsunobuchi, Y.; Matsuda, T.; Hashimoto, K.; Namai, A.; Hakoe, F.; Tokoro, H. *Nat. Chem.* **2010**, *2*, 539.
(4) Ueda, H.; Kitazawa, K.; Takagi, H.; Matsumoto, T. *J. Phys. Soc. Jpn.* **2002**, *71*, 1506.
(5) Watanabe, M.; Miyasaka, M.; Tanaka, K. *J. Phys. Conf. Ser.* **2009**, *148*, 012017.
(6) Smith, J. R.; Walsh, F. C.; Clarke, R. L. *J. Appl. Electrochem.* **1998**, *28*, 1021.
(7) Walsh, F. C.; Wills, R. G. A. *Electrochim. Acta* **2010**, *55*, 6342.
(8) Doherty, C. M.; Caruso, R. A.; Smarsly, B. M.; Adelhelm, P.; Drummond, C. J. *Chem. Mater.* **2009**, *21*, 5300.
(9) Minakuchi, H.; Nakanishi, K.; Soga, N.; Ishizuka, N.; Tanaka, N. *Anal. Chem.* **1996**, *68*, 3498.
(10) Núñez, O.; Nakanishi, K.; Tanaka, N. *J. Chromatogr. A* **2008**, *1191*, 231.
(11) Hench, L. L. *J. Am. Ceram. Soc.* **1991**, *74*, 1487.
(12) Breulmann, M.; Davis, S. A.; Mann, S.; Hentze, H. P.; Antonietti, M. *Adv. Mater.* **2000**, *12*, 502.
(13) Maekawa, H.; Esquena, J.; Bishop, S.; Solans, C.; Chmelka, B. F. *Adv. Mater.* **2003**, *15*, 591.
(14) Drisko, G. L.; Zelcer, A.; Luca, V.; Caruso, R. A.; Soler-Illia, G. J. d. A. A. *Chem. Mater.* **2010**, *22*, 4379.
(15) Fan, X.; Fei, H.; Demaree, D. H.; Brennan, D. P.; St. John, J. M.; Oliver, S. R. J. *Langmuir* **2009**, *25*, 5835.
(16) Kanamori, K.; Nakanishi, K. *Chem. Soc. Rev.* **2011**, *40*, 754.
(17) Tokudome, Y.; Fujita, K.; Nakanishi, K.; Miura, K.; Hirao, K. *Chem. Mater.* **2007**, *19*, 3393.
(18) Tokudome, Y.; Fujita, K.; Nakanishi, K.; Kanamori, K.; Miura, K.; Hirao, K.; Hanada, T. *J. Ceram. Soc. Jpn.* **2007**, *115*, 925.
(19) Konishi, J.; Fujita, K.; Nakanishi, K.; Hirao, K. *Chem. Mater.* **2006**, *18*, 864.
(20) Hasegawa, G.; Kanamori, K.; Nakanishi, K.; Hanada, T. *J. Am. Ceram. Soc.* **2010**, *93*, 3110.
(21) Ruzimuradov, O.; Hasegawa, G.; Kanamori, K.; Nakanishi, K. *J. Am. Ceram. Soc.* **2011**, *94*, 3335.
(22) Konishi, J.; Fujita, K.; Oiwa, S.; Nakanishi, K.; Hirao, K. *Chem. Mater.* **2008**, *20*, 2165.
(23) Nakanishi, K.; Tanaka, N. *Acc. Chem. Res.* **2007**, *40*, 863.
(24) Kolbrecka, K.; Przyluski, J. *Electrochim. Acta* **1994**, *39*, 1591.
(25) Toberer, E. S.; Weaver, J. C.; Ramesha, K.; Seshadri, R. *Chem. Mater.* **2004**, *16*, 2194.
(26) Burdett, J. K.; Hughbanks, T.; Miller, G. J.; Richardson, J. W.; Smith, J. V. *J. Am. Ceram. Soc.* **1987**, *109*, 3639.
(27) Rice, C. E.; Robinson, W. R. *Mater. Res. Bull.* **1976**, *11*, 1355.
(28) Asbrink, S.; Magneli, A. *Acta Crystallogr.* **1959**, *12*, 575.
(29) Le Page, Y.; Strobel, P. *J. Solid State Chem.* **1982**, *43*, 314.
(30) Rao, C. N. R.; Ramdas, S.; Loehman, R. E.; Honig, J. M. *J. Solid State Chem.* **1971**, *3*, 83.

(31) Honig, J. M.; Reed, T. B. *Phys. Rev.* **1968**, *174*, 1020.
(32) Paunović, P.; Popovski, O.; Fidanevska, E.; Ranguelov, B.; Stoevska Gogovska, D.; Dimitrov, A. T.; Hadi Jordanov, S. *Int. J. Hydrogen Energy* **2010**, *35*, 10073.
(33) Rashkova, V.; Kitova, S.; Vitanov, T. *Electrochim. Acta* **2007**, *52*, 3794.
(34) Ioroi, T.; Siroma, Z.; Fujiwara, N.; Yamazaki, S. I.; Yasuda, K. *Electrochem. Commun.* **2005**, *7*, 183.
(35) Chen, G.; Bare, S. R.; Mallouk, T. E. *J. Electrochem. Soc.* **2002**, *149*, A1092.
(36) Scott, K.; Taama, W.; Cheng, H. *Chem. Eng. J.* **1999**, *73*, 101.
(37) Chen, G.; Betterton, E. A.; Arnold, R. G.; Ela, W. P. *J. Appl. Electrochem.* **2003**, *33*, 161.